2007 Urban Remote Sensing Joint Event

Cell Decomposition for Building Model Generation at Different Scales

Norbert Haala, Susanne Becker, Martin Kada
Institute for Photogrammetry
Universität Stuttgart
Germany
forename.lastname@ifp.uni-stuttgart.de

***Abstract*— Usually, 3D building reconstruction is realized by systems, which either apply constructive solid geometry (CSG) or boundary representation (B-Rep) to model the respective buildings. We present an alternative approach based on cell decomposition, which can be used efficiently for building reconstruction at different scales. Firstly, building polyhedrons are constructed from airborne LIDAR data and given outlines of the respective buildings. In this context, cell decomposition is used to guarantee topological correct representations and the simple implementation of constraints between different building parts like coplanarity or right angles. As it will be demonstrated in the second part of the paper, cell decomposition is also advantageous if large scale building models have to be generated for example based on the analysis of terrestrial LIDAR data.**

I. INTRODUCTION

The automatic and semiautomatic collection of 3D building models can be realized by a number of algorithms. During data collection, the polyhedral building models are either represented using a constructive solid geometry (CSG) or a boundary representation (B-Rep) based approach. Within B-Rep approaches the planar surface boundaries of the 3D building objects to be reconstructed are directly generated from the vertices, edges or faces, which are for example measured from airborne LIDAR or stereo imagery. However, while numerous approaches are available for the extraction of such primitives to be used as building fragments, the combination of these segments to generate topological correct boundary representations is difficult to implement [1]. This task is additionally aggravated if geometric constraints, such as meeting surfaces, parallelism and rectangularity have to be guaranteed for such measured and thus error-prone fragments.

In contrast, these regularization conditions can be met easier, if object representations based on CSG are used [2]. Within CSG based modeling, simple primitives are combined by means of regularized Boolean set operators. An object is then stored as a tree with the primitives as the leaves and operators at internal nodes. Some nodes represent Boolean operators like union or intersection, or set difference, whereas others perform translation, rotation and scaling. Since modeling using primitives and Boolean operations is much more intuitive than specifying B-Rep surfaces directly, CSG is used widely in computer aided design [3]. CSG representations are also always valid since the simple primitives are topologically correct and this correctness is preserved during their combination by the Boolean operations. Additionally, the implicit geometrical constraints of these primitives like parallel or normal faces of a box type object allows for the quite robust parameter estimation. This is especially important for reconstructions based on error prone measurements. However, suitable object representation requires the availability of an appropriate set of primitives, which can be difficult for complex buildings.

Fig. 1 exemplarily gives the result for a CSG based algorithm [4]. This fully automatic reconstruction is based on the decomposition of a given ground plan into rectangles by a heuristic algorithm. For each of these rectangles, an optimal 3D primitive is selected from a fixed set of available roof types (flat, hipped, ridge and desk). This selection as well as the respective parameter estimation is based on the fit to the original roof surface measured by airborne LIDAR data. A semiautomatic extension can additionally be used to modify the fully automatic primitive selection and parameter estimation.

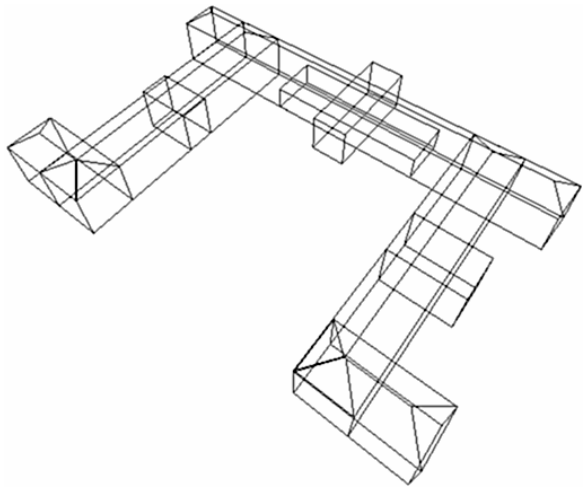

Figure 1. Building representation by constructive solid geometry

Most visualization and simulation applications require the derivation of a boundary representation from the collected CSG model. For this reason also the 3D primitives depicted in Fig. 1 are combined by a Boolean merge operation to generate the final building model. Conceptually, this so-called boundary

evaluation can be realized easily. However, its correct and efficient implementation can be difficult since error-prone measurements, problems of numerical precision and unstable calculation of intersections can considerably hinder the robust generation of a valid object topology. The difficulties to provide robust implementations seem to be rooted in the interaction of approximate numerical and exact symbolic data [5].

These problems can be facilitated by the concept of cell decomposition, which is also well known in solid modeling. Similar to CSG complex solids are described by a combination of relatively simple, basic objects in a bottom up fashion. In contrast to CSG, decomposition models are limited to adjoining primitives. Since the basic primitives must not intersect they are thus 'glued' together to get the final model. This step can be interpreted as a restricted form of a spatial union operation. In this sense cell decomposition is similar to a spatial occupancy enumeration, where the object space is subdivided by non overlapping cubes of uniform size and orientation. However, cell decompositions are based on a variety of basic cells, which may be any objects that are topologically equivalent to a sphere i.e. do not contain holes. This allows for a simplified combination of the respective elements, while the disadvantages of exhaustive enumeration like large memory consumption and the restricted accuracy of the object representation can be avoided. Usually, cell decomposition is used within solid modeling applications as auxiliary representation for specific computations [3]. However, it can be applied efficiently for the automatic reconstruction of topological correct building models at different levels of detail. This concept of cell decomposition for the representation of a 3D building is demonstrated in Fig. 2.

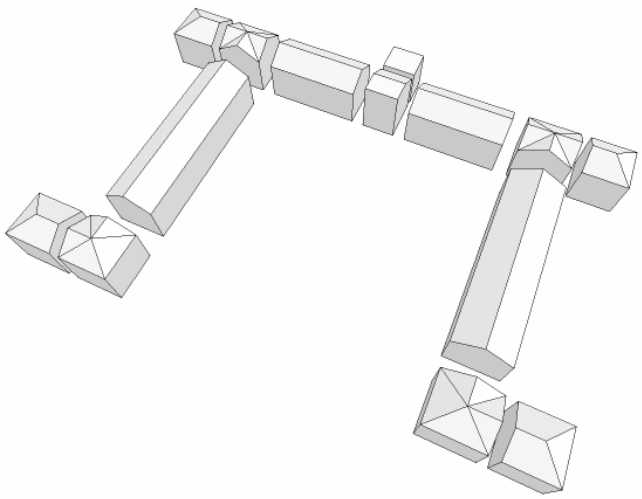

Figure 2. Building representation by cell decomposition

In the following section our cell decomposition approach for the reconstruction of polyhedral 3D building models by a suitable subdivision of space into 3D primitives is discussed. As input data a 2D building ground plan and a triangulated 2.5D point cloud from airborne laser scanning are used. As first step, a set of space dividing planes is derived, which generates a set of primitives that organize the infinite space into building and non-building parts. After these building primitives are glued together, the resulting 3D building model is a good approximation of the real world object. As discussed within section III, this representation can be refined in an additional step by the integration of 3D points as collected by terrestrial laser scanning. By these means façade structure like window areas or protrusions can additionally be modeled.

II. BUILDING RECONSTRUCTION FROM GIVEN GROUND PLANS AND AIRBORNE LIDAR

An approximation of the 3D building can be generated easily by a simple extrusion of the 2D ground plan. The vertical extension of this 3D building object can be determined from the airborne LIDAR measurements within the building footprint. A more detailed representation of the building roof can in principle be generated additionally by triangulation of these 3D points. However, as demonstrated in Fig.3 the visual quality of such a building model from directly triangulated LIDAR points is not adequate for most applications. This is mainly due to deviations between the piecewise flat parts of the roof and their approximation by a meshed surface.

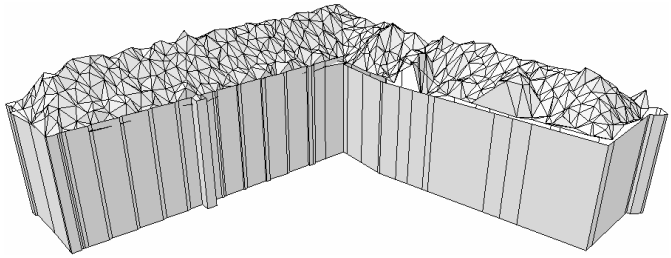

Figure 3. Extruded ground plan and meshed LIDAR data

Frequently, algorithms for the generation of polygonal or triangular meshes also allow for a smoothing of the originally measured 3D point clouds. Additionally, surface simplification can be used to generate geometric object representations at different levels of detail, while the original shape is preserved by suitable optimization criteria. A number of such approaches have been developed in computer graphics, which are very suitable for general objects. However, they are not adequate to preserve special characteristics like right angles or parallel lines as they occur frequently at man-made objects such as buildings. If the aforementioned features are not maintained during surface modelling, the quality of the resulting building model will be limited significantly. For this reason a number of approaches for 3D building reconstruction first extract planar regions of appropriate size from the originally measured 3D points. Polyhedral building models are then generated by intersection of the segmented regions, while regularization constraints as derived from the building architecture are guaranteed. However, such a direct generation of a constrained boundary representation can become highly complex. In contrast, a decomposition of the extruded ground plan for the generation of initial 3D cells can help to facilitate these problems.

A. Construction of decomposition cells

During the extrusion process for each segment of the ground plan a polygonal face perpendicular to the horizontal building footprint is generated, which is then used for our cell

decomposition process. Despite the application of 3D features, 2D sketches are used for easier illustration of the approach in Fig.4 and 5. Within these figures the planes perpendicular to the horizontal ground plan as generated by the extrusion process are depicted as straight lines while the 3D objects are represented by their horizontal footprints. In order to additionally allow for a scale dependent generalization, planar buffers are used within the subdivision process. This buffer includes protrusions and other small structural elements, which can optionally be eliminated before further processing. Thus, the number of planes, which are required to approximate the final 3D model, can be minimized.

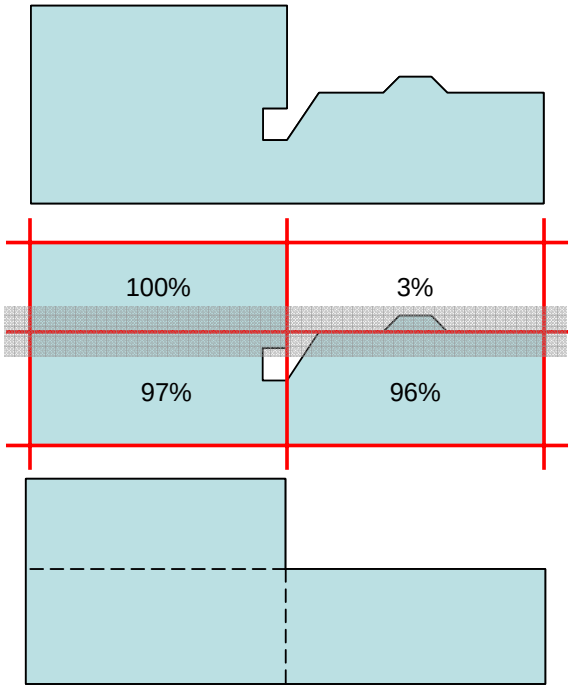

Figure 4. Approximation of 2D building ground plan by subdivision planes

This process is illustrated in Fig. 4. While the given ground plan is depicted at the top, the six vertical subdivision planes are shown as the red lines in the middle image. Additionally, for one subdivision plane the respective buffer area is represented by the grey region. The generated subdivision planes are then used to decompose the 3D space. Since the required computations are impractical for an infinite space, they are limited to a solid two times the size of the building's bounding box. The result of the subdivision is a set of solid blocks, which have to be differentiated in building and non-building primitives in a subsequent step. For this purpose a percentage value is calculated for each primitive that denotes the volume of the original building model inside the respective block. All solids with a percentage value under a given threshold value are then denoted as non-building primitives and are discarded from further processing. Because the primitives are rather coarse, a threshold value of around 50% is suitable in most cases. When glued together as depicted in the bottom image of Fig. 4, the building blocks form a flat-top approximation that is shaped after the original ground plan. The process of cell generation and selection for the ground plan already used in Fig. 3 is demonstrated in Fig. 5. The top image shows the generated subdivision planes as a vertical view. The building cells, which were selected due to their overlap with the given ground plan, are marked in red. Within the 3D bottom view, these 3D cells are represented by the grey solids. Additionally, the extruded ground plan is depicted in red.

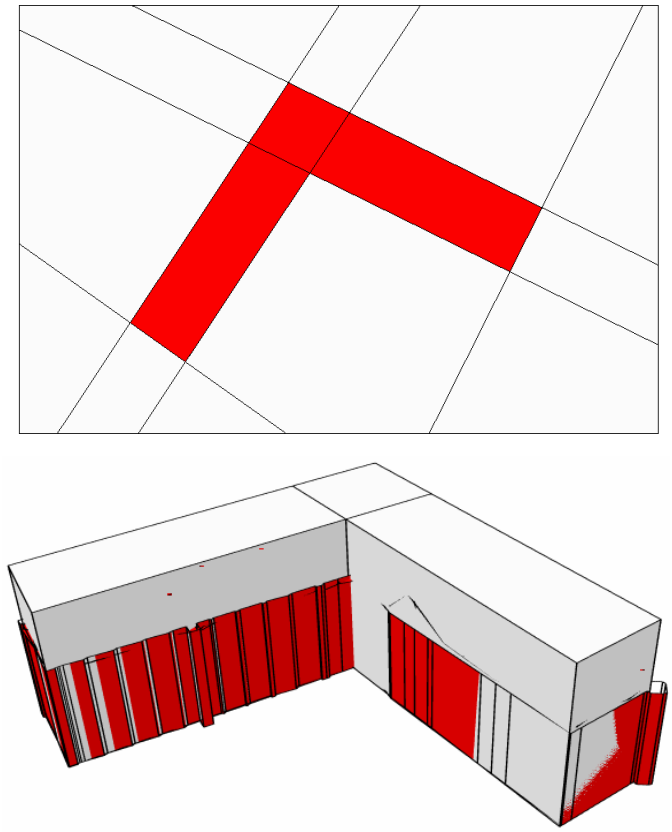

Figure 5. Building cells generated from ground plan analysis

B. Roof reconstruction from airborne LIDAR

The vertical extensions of the 3D cells and the extruded ground plan were determined from the 3D LIDAR points within the building footprint. While the lowest point defined the height of the extruded ground plan, the highest value provided the upper bound of the 3D cells. Within a second step, a combined analysis of these 3D flat-top building cells and the measured LIDAR points is used to reconstruct a suitable roof structure for the respective building fragments. For this purpose, an iterative generation of subdivision planes is based on the meshed triangles as derived from the measured LIDAR points. Similar to a process described in [6] each TIN mesh defines a planar surface at the start of a merging process. Within this process, coplanar surfaces are iteratively merged and the plane equation is updated until no more similar surfaces can be found.

Although the cell decomposition process based on the extruded ground plan generates individual building blocks, the planes for roof reconstruction are determined globally from the triangulated 2.5D point cloud. This ensures that the resulting roof polygons still fit against each other at neighboring blocks. Fig. 6 shows the original 3D cells as they are partitioned by the

subdividing planes as they are generated by analysis of the meshed surface from LIDAR measurements.

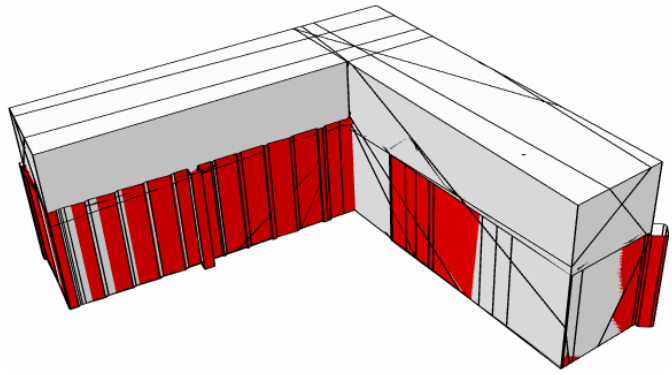

Figure 6. Decomposition planes for roof reconstruction.

Similar to the cell decomposition process described in the previous section, roof cells have to be separated from non-roof segments in the following step. For this purpose, the 3D reconstruction from the meshed LIDAR points depicted in Fig. 3 is used. Each of the potential 3D roof cells depicted in Fig. 6 is intersected with the 3D building object in Fig. 1. A 3D cell is selected if there is a sufficient overlap in 3D object space, i.e. if a solid lies within the approximated building object of Fig. 1.

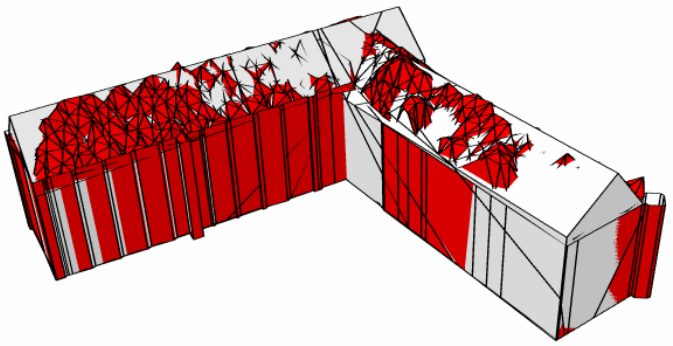

Figure 7. Selected 3D building cells overlaid to meshed LIDAR points.

The selected cells are shown as grey solids within Fig. 7. For comparison the building object from the extruded ground plan and meshed LIDAR data, which is already shown in Fig. 1 is drawn in red. To shape the final 3D building model these selected cells are glued together in a simple spatial union operation.

III. Modeling of Façades from Terrestrial LIDAR

The airborne LIDAR data used for the exemplary reconstruction in the previous section were collected at a mean point distance of 1,5m. This prevents a very detailed reconstruction of the respective roof. However, the general structure of the building is captured successfully. This type of reconstruction, which is typical for airborne data collection, is sufficient for a number of applications. Nevertheless, some tasks like the generation of realistic visualizations from pedestrian viewpoints require an increased quality and amount of detail for the respective 3D building models. This can be achieved by terrestrial images mapped against the facades of the buildings. However, this substitution of geometric modeling by real world imagery is only feasible to a certain degree. Thus, for a number of applications a geometric refinement of the building facades will be necessary. As an example, protrusions at balconies and ledges, or indentations at windows will disturb the visual impression if oblique views are generated. As it will be demonstrated by the integration of window objects, our approach based on cell decomposition is also well suited for such a geometric refinement of an existing 3D model.

A. Data pre-processing

Densely sampled point clouds from terrestrial laserscanning provide a considerable amount of geometric detail and can therefore be used well for the enhancement of building façades. Frequently such data are collected from multiple viewpoints to avoid occlusions and guarantee complete object coverage. Thus, the different scans have to be co-registrated and geocoded as a first processing step. Traditionally, the required control point information is provided by measurement of specially designed targets. Alternatively, an approximate direct georeferencing can be combined with an automatic alignment to existing 3D building models [7]. After geocoding, the 3D point cloud and the building models are available in a common reference system. Thus, relevant 3D point measurements can be selected easily for each part of the building.

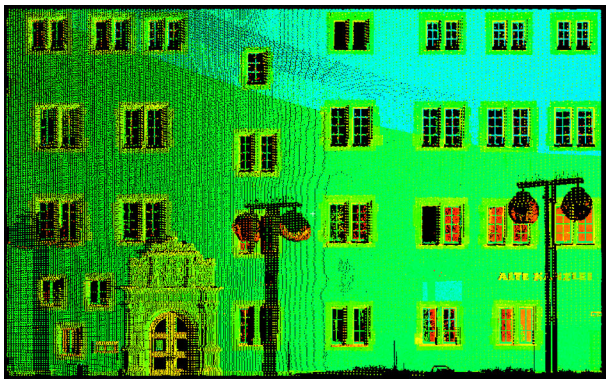

Figure 8. Façade plane with corresponding 3D point cloud.

For our investigations 3D points were collected by terrestrial laser scanning at an approximate spacing of 4cm. Fig. 8 shows a part of this point cloud, which was extracted for a façade plane by a simple buffer operation. The geometric alignment of the 3D points and the respective building façade also allows for a mapping of the points to this reference plane. Afterwards, further processing is simplified to a 2.5D problem.

B. Segmentation of façade cells

Depending on the angle of incidence, point measurements at the window glass are either prevented due to specular reflection or, if the beam is not reflected, refer to points behind. Thus, as it is also visible in Fig. 8 no 3D points are available at window areas. Of course, point measurement at such a façade can also be prevented by occlusions. However, since point clouds are collected from different viewpoints, occluding objects only reduce the number of LIDAR points while a number of measurements are still available from the other viewpoints.

For these reasons in the following step, LIDAR points measured at window borders are used to generate 3D cells, which either represent a homogenous part of the façade or an empty space in case of a window. After they have been differentiated based on the availability of measured LIDAR points, empty cells are eliminated from the facade, while the remaining façade cells are glued together to generate the refined 3D building model.

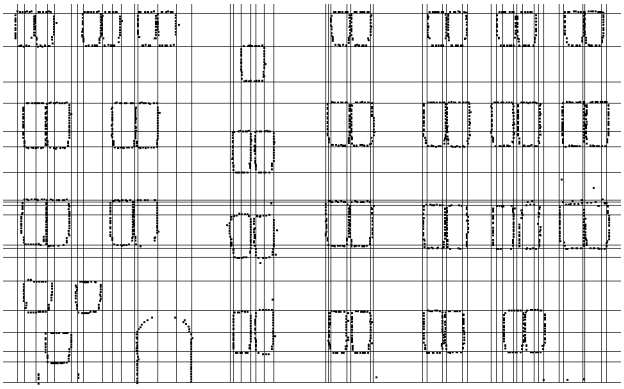

Figure 9. Detected edge points with generated window lines.

Fig. 9 depicts the edge points extracted by our segmentation algorithm. During this segmentation step four different types of window borders are distinguished: horizontal structures at the top and the bottom of the window, and two vertical structures that define the left and the right side. As an example, to extract edge points at the left border of a window, points with no neighbor measurements to the right have to be detected. In this way, four different types of structures are detected in the LIDAR points of Fig. 8. In addition to these extracted points Fig. 9 depicts horizontal and vertical lines, which can be estimated from non-isolated edge points. Each of these lines can be used to define a plane, which is perpendicular to the building façade. Thus, similar to the ground plan fragmentation in section II, these planes provide the basic structure of the 3D cells to be generated. All these cells are then separated into building and non-building fragments using a binary 'point-availability-map' depicted in Fig.10.

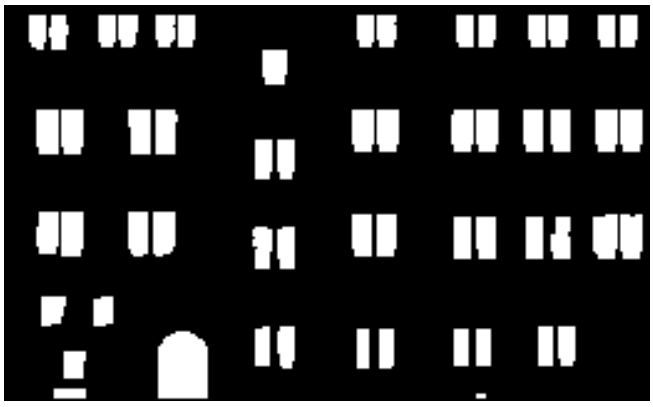

Figure 10. Point-availability-map.

Within this image, black pixels are grid elements where LIDAR points are available. In contrast, white pixels define raster elements with no 3D point measurements. Of course, the already extracted edge points and structures in Fig. 9 are more accurate than this rasterized image. However, this limited accuracy is acceptable since the binary image is only used for classification of the 3D cells by computing the respective ratio of façade to non-façade pixels for each cell. This process corresponds to the separation of building and non building cells by ground plan analysis as shown in Fig.4 and 5.

C. Elimination of window cells

As it is depicted in Fig.11, façade cells can be integrated easily within the approximate building model if necessary. This is realized by intersecting the planes generated from the window lines in Fig. 9 with the façade plane and an additional plane behind the façade at window depth. This depth is derived from LIDAR measurements at window cross bars, which are detected by a search plane parallel to the façade shifted in its normal direction.

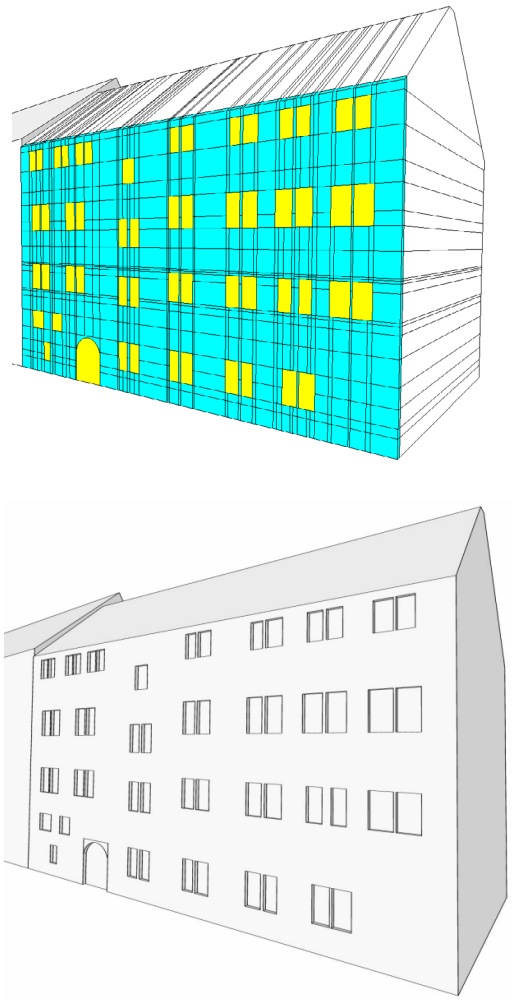

Figure 11. Refined facade of the reconstructed building.

The top image of Fig. 11 depicts the 3D cells of the coarse building model based on the extracted window lines. Façade cells are marked in blue, while window cells are marked as yellow. These window cells are then removed to generate the final

model depicted in the bottom image. While the windows are represented by polyhedral cells, also curved primitives can be integrated in the reconstruction process. This is demonstrated exemplarily by the round-headed door of the building.

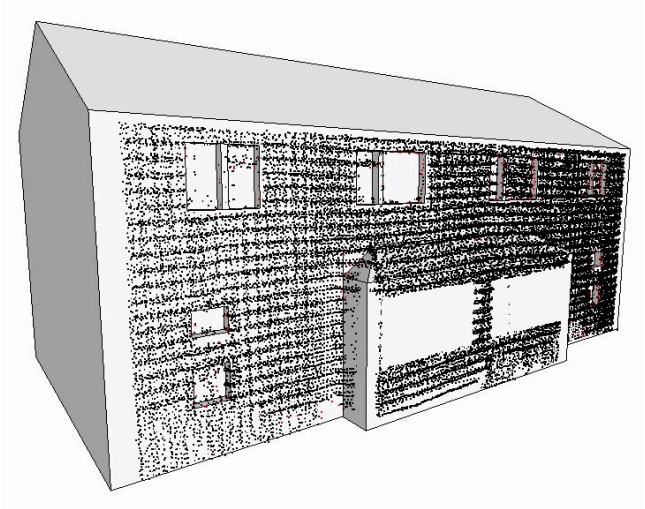

Figure 12. Refined building model with added protrusion

Fig. 12 gives an additional example of model refinement based on terrestrial LIDAR measurement, were in addition to the elimination of window cells a protrusion was added in the refinement step.

IV. CONCLUSION

Within the paper, an approach for 3D building reconstruction using 2D ground plans and 3D point clouds from airborne and terrestrial LIDAR is presented. The basic idea of the approach is to subdivide the 3D space into general polyhedral 3D primitives by cell decomposition. For this purpose, sets of space dividing planes separate the infinite space into building and non-building parts. These intersecting planes are derived from the segments of the given ground plan. Within this step, buffer operations are used. Thus, the extruded ground plans can be simplified by the selection of a suitable buffer size. Usually, this parameter will be determined in accordance to the point density from airborne LIDAR measurement, which is used for the integrated roof reconstruction. In this respect, the reconstruction of the 3D building shape from 2D ground plan and LIDAR measurement is similar to a generalisation approach presented in [8]. There, the 3D geometry of polygonal building blocks from an existing 3D urban model is simplified. For both tasks, the use of cell decomposition enables the generation of building models at multiple scales. Simultaneously, the preservation of symmetry relations like coplanarity can be guaranteed comparatively easy by using constraints for the respective subdivision planes. Finally, the 3D building primitives can be combined easily, since the generated cells do not intersect.

Even though the resulting 3D building model is a good approximation of the real world object, further refinement based on additional detail from terrestrial LIDAR data is possible. This flexible integration of object parts could be demonstrated for windows, which are represented by indentations. However, a reconstruction based on cell decomposition can for example also be used to efficiently subtract rooms from an existing 3D model if measurements in the interior of the building are available. Although algorithmic improvement is still feasible, in our opinion the concept of generating 3D cells by the mutual intersection of planes has already proved to be very promising and has a great potential for the reconstruction of building models at multiple scales.

ACKNOWLEDGMENT

The research described in this paper is founded by “Deutsche Forschungsgemeinschaft” (DFG – German Research Foundation). It takes place within the Centre of Excellence No. 627 “NEXUS – SPATIAL WORLD MODELS FOR MOBILE CONTEXT AWARE APPLICATIONS” at the Universiaet Stuttgart.

REFERENCES

[1] Rottensteiner, F., *Semi-automatic extraction of buildings based on hybrid adjustment using 3D surface models and management of building data in a TIS* 2001. PhD thesis, TU Wien .

[2] Brenner, C., "Modelling 3D Objects Using Weak CSG Primitives," *IAPRS Vol. 35*, 2004.

[3] Mäntylä, M. *An Introduction to Solid Modeling*, Computer Science Press, Maryland, U.S.A. 1988.

[4] Haala, N. and Brenner, C., Virtual City Models from Laser Altimeter and 2D Map Data *Photogrammetric Engineering & Remote Sensing*, vol. 65, pp. 787-795, 1999.

[5] Hoffmann, C. M. *Geometric & Solid Modelling*, San Mateo, CA: Morgan Kaufmann Punblishers, Inc., 1989.

[6] Gorte, B., "Segmentation of TIN-Structured Surface Models," *Proceedings Joint International Symposium on Geospatial Theory, Processing and Applications*, 2002.

[7] Böhm, J. and Haala, N., "Efficient Integration of Aerial and Terrestrial Laser Data for Virtual City Modeling Using LASERMAPS," *IAPRS Vol. 36 Part 3/W19 2005* ,pp. 192-197, 2005.

[8] Kada, M., "3D building generalization based on half space modelling," *Joint ISPRS Workshop on Multiple Representation and Interoperability of Spatial Data*, 2006.